Density Functional Study of Intradimer Proton Transfers in Hydrated Adenine Dimer Ions, $A_2^+(H_2O)_n$ ($n = 0-2$)

Hye Sun Park, Sang Hwan Nam, Jae Kyu Song, Seung Min Park,* and Seol Ryu*

Department of Chemistry, Kyunghee University, Seoul 130-701, Republic of Korea

Received: February 12, 2008; Revised Manuscript Received: June 25, 2008

Structures of mono- and dihydrated adenine dimers and their cations were calculated using B3LYP density functional theory with the 6-31+G(d,p) basis set, in order to help understand photofragmentation experiments of hydrated adenine dimers from the energetics point of view. Several important pathways leading to the major fragmentation product, protonated adenine ion (AH^+), thermodynamically at minimum costs were investigated at the ground-state electronic potential surface of hydrated adenine dimer cations. Our calculations suggest that the proton transfer from one adenine moiety to the other in hydrated dimer ions readily occurs with negligible barriers in normal hydration conditions. In asymmetrically hydrated ions, however, the proton transfer to more hydrated adenine moieties is kinetically hindered due to heightened transition-state barriers, while the other way is still barrierless. Such directional preference in proton transfer may be characterized as a unique dimer ion property, stemming from the difference in basicity of the two nitrogen atoms involved in the double hydrogen bond that would be equivalent without hydration. We also found that dimer cleavage requires about 4 times larger energy than evaporation of individual water molecules, so it is likely that most solvent molecules evaporate before the eventual dimer cleavage when available internal energy is limited.

I. Introduction

In normal biological systems, DNA strands contain the sequences coded with the four major bases for genetic information to be carried down generations, so it is inferred that the DNA bases exhibit strong stability against electromagnetic radiation. Indeed, a significant amount of recent literature on gas-phase studies has indicated that the lifetimes of the excited states of individual DNA bases upon UV/vis absorption are sufficiently short,[1−7] while mutation may be triggered in the excited states. Such photochemical properties of DNA bases may protect genetic information from mutagenic damage. In vivo, however, DNA bases are hydrated to the full extent at considerable ionic strengths as well as being stacked and paired with each other in the double strands, which may give DNA bases in actual biological environments at least quantitatively different photochemical properties from those observed from single DNA-base molecule photoexcitations.[4−7] Therefore, one may consider DNA base pairs, presumably hydrated with several water molecules, as the next simple model units to be tested for photostability, due to their close resemblance with actual biological systems in terms of base pairing and hydration.

Homopaired adenine has been studied by several groups[8−12] not only because it is structurally similar to the double-hydrogen-bonded adenine−thymine pair but also because of the well-studied photochemistry of adenine[13−20] and because the relatively easy preparation of homopaired bases make it possible to discern unique photochemical properties originating only from dimer formation of base molecules. As far as photochemical damages are concerned, proton transfer reactions play important roles because one of the common consequences upon photoexcitations is the appearance of protonated products, which has been suggested to cause mutation.[21] The monomeric properties of protonated adenines and their dissociation mechanisms have been studied by several groups.[22−24] Recently, it was suggested that protonated adenines are produced both by proton transfer in adenine dimer ions and by hydrogen transfer in the electronically excited state of neutral adenine dimer.[25]

In our previous work,[12] photodissociation experiments of hydrated adenine dimers showed, upon photoexcitation at wavelengths 532 and 355 nm, that the major fragment from hydrated adenine dimer ions, $(A-A)^+(H_2O)_n$, ($n = 0-6$), is protonated adenine monomer ions, AH^+, while no hydrated monomer ions, $A^+(H_2O)_n$, are observed. It was claimed that proton transfer *between adenine monomers* would promptly follow the ionization of dimers with only small internal energies available at the ground-state potential energy surface, and then, as soon as some chromophore species of the hydrated ions are provided with extra energy, most of the water molecules would evaporate sequentially until the dimer ion eventually cleaves into the protonated adenine, AH^+, and the dehydrogenated adenine radical, A−H.

In principle, such complicated protonation dynamics can ideally be studied by ab initio molecular dynamics simulation taking into account both the excited states and the ground state;[26−29] however, high computational costs make such a simulation for much hydrated systems virtually unrealistic to date. From a practical point of view, therefore, it is better to distinguish the ground-state dynamics of ionic species from the excited-state dynamics and study both issues separately.

In this work, we will theoretically quantify the intradimer proton transfer of hydrated adenine dimer ions and the effects of hydration in both kinetic and thermodynamic perspectives. Although our discussion here will be restricted to the energetics at the ground-state potential surfaces, following a rather simple reaction scheme, $A_2(H_2O)_n \rightarrow A_2^+(H_2O)_n \rightarrow [AH^+-(A-H)](H_2O)_n \rightarrow AH^+ + (A-H) + nH_2O$ ($n = 0-2$), a theoretical case study is expected to provide us general and quantitative

* To whom correspondence should be addressed. Tel: 82-2-961-0237. Fax: 82-2-966-3701. E-mail: smpark@khu.ac.kr (S.M.P.), sryu@khu.ac.kr (S.R.).

10.1021/jp801238b CCC: $40.75
Published on Web 08/30/2008

insights into the overall photofragmentation processes of hydrated adenine dimers,[12,29,30] and help clarify excited-state dynamics.

In the next section, we will explain the computational methods employed. Then, we will present mono- and dihydration patterns of neutral adenine dimers and discuss the energetics as they undergo ionization, intradimer proton transfer, evaporation, and dimer cleavage, with the focus on effects of hydration on each process. We summarize our work in the final section.

II. Calculation Details

We used Gaussian 03 quantum chemistry suite[31] for all calculation results presented in this work. All calculations were done at the level of B3LYP density functional with the 6-31+G(d,p) basis set, as a few test calculations with the large basis set 6-311++G(d,p) led to improvements of only 3% or less in energies, preserving all other physical contents nearly unaltered. For intradimer proton transfer reactions, we first optimized hydrated dimer ion structures before and then after proton transfer. Transition-state molecular configurations connecting the two kinds of structures were found using the quadratic synchronous transit method implemented in Gaussian 03. To confirm the transition states, we checked on a single imaginary frequency mode of each of them and utilized intrinsic reaction coordinate (IRC) calculations as well. At the optimized geometries, harmonic vibrational frequencies were calculated and used for correcting molecular electronic energies without scaling them. In addition, the natural bond orbital (NBO) charges were evaluated using natural population analysis.[32] For calculations of dissociation energies for evaporation and dimer cleavage, counterpoise corrections were carried out to reduce the basis-set superposition error.[33]

III. Results and Discussion

A. Hydration Patterns for Adenine Dimers. While both hydration patterns for a single adenine molecule and structures of adenine dimers have been studied extensively,[8−11,34−40] structures of hydrated adenine dimers were not investigated as much. To figure out hydrated adenine dimer structures in the neutral states first, we considered various dimer structures in which one or two hydrogen bonds can couple two adenine molecules. A single adenine molecule has three major sites, μ, ν, and ξ, available for hydrogen bonding,[36,37] as shown in the top of Figure 1, and among many possible combinations via different hydrogen-bonding sites of the two adenine molecules to make a dimer, it has been reported that two parallel hydrogen bonds, a double hydrogen bond, between two monomers result in six most stable adenine dimers.[8,9] We confirmed the six adenine dimers at the B3LYP/6-31+G(d,p) level. (Figure S1, Supporting Information) It is noteworthy that the most stable dimer structure is the one where the double hydrogen bond is made via ξ sites of the two adenine monomers, and it is about 3.5 kcal/mol lower in energy than the next stable one. We will refer to it as the $\xi\xi'$ dimer structure (or simply dimer) and consider hydration patterns for this structure only, so holding the number of subsequent reaction processes manageable as we discuss ionization, proton transfer, and dehydration in the following subsections. The prime is used for referring to the second adenine molecule or the sites belonging to it. The second adenine will be usually the one on the right-hand side in figures where the dimer structures appear. This convention will be used throughout this work.

Now, we consider hydration cases of the neutral adenine dimer $\xi\xi'$. (Optimized geometries are showed in Supporting Information, Figure S2, and their energies are listed in Table 1.) The $\xi\xi'$ dimer has two nonequivalent hydration sites, μ and ν, so the corresponding monohydrated structures are called μ-$\xi\xi'$ and ν-$\xi\xi'$, respectively. The prefixes denote the hydration positions of the water molecule. ν-$\xi\xi'$ is 1.8 kcal/mol more stable than μ-$\xi\xi'$, consistent with the previous calculation that ν is a more favored hydrogen-bonding site than μ.[37]

In the same way, we construct neutral dihydrated dimer structures as follows, $\mu\mu$-$\xi\xi'$, $\nu\nu$-$\xi\xi'$, $\mu\nu$-$\xi\xi'$, $\nu\mu'$-$\xi\xi'$, $\mu\mu'$-$\xi\xi'$, and $\nu\nu'$-$\xi\xi'$. The relative energies between dihydrated dimer structures are within 3.5 kcal/mol, and the ordering of structures in energy reflects the degree of each site being favored as a hydrogen-bonding site. In unilateral hydration cases, $\nu\nu$-$\xi\xi'$ is more stable than $\mu\mu$-$\xi\xi'$, because the ν site is more favored than the μ site, and $\mu\nu$-$\xi\xi'$ goes between the two. Interestingly, in cases of bilateral dihydration, in which the two water molecules are bonded separately to the two different adenine monomers, the hydrated structures are even more stabilized. For instance,

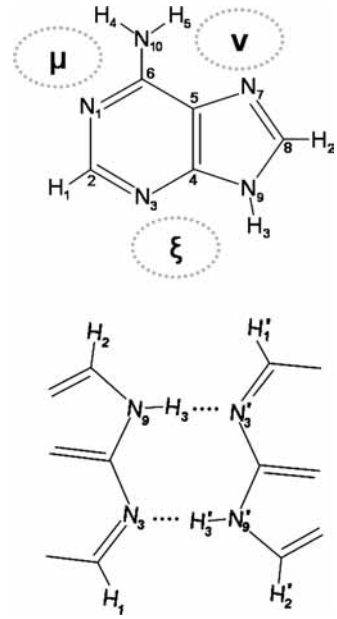

Figure 1. (Top) Adenine molecule with the three major hydrogen-bonding sites, μ, ν, and ξ, indicated. (Bottom) The double hydrogen bond formed between two adenine monomers via the mutually equivalent sites ξ and ξ'. The primed letter is used to indicate a site at the other monomer on the right-hand side, and so this dimer is called, $\xi\xi'$. The H_3 atom is often referred to as 9H, since it is bonded to N_9 of the five-membered ring.

TABLE 1: Vertical and Adiabatic Ionization Energies (eV) for Hydrated Adenine Dimer at the B3LYP/6-31+G(d,p) Level

		ionization energy			
	neutral[a]	vertical	adiabatic	difference	ion[a]
$\xi\xi'$	−934.5078	7.76	7.67	−0.09	−934.2258
μ-$\xi\xi'$	−1010.9317	7.79	7.56	−0.23	−1010.6540
ν-$\xi\xi'$	−1010.9345	7.75	7.59	−0.16	−1010.6556
$\mu\mu$-$\xi\xi'$	−1087.3575	7.76	7.57	−0.19	−1087.0793
$\nu\nu$-$\xi\xi'$	−1087.3587	7.75	7.58	−0.17	−1087.0802
$\mu\nu$-$\xi\xi'$	−1087.3578	7.79	7.45	−0.34	−1087.0839
$\nu\mu'$-$\xi\xi'$	−1087.3583	7.78	7.51	−0.27	−1087.0822
$\mu\mu'$-$\xi\xi'$	−1087.3556	8.16	7.49	−0.67	−1087.0803
$\nu\nu'$-$\xi\xi'$	−1087.3612	7.74	7.54	−0.20	−1087.0842

[a] The energies in au for the optimized structures of hydrated adenine dimer in neutral and ionic states are also listed for comparison.

the symmetrically and bilaterally dihydrated dimer, $\nu\nu'$-$\xi\xi'$, is even more stable than the doubly and unilaterally dihydrated dimer, $\nu\nu$-$\xi\xi'$. To explain a few terms to classify dihydrated adenine dimers, first, the laterality refers to the number of adenine monomers hydrated. Second, by "doubly", we mean that two water molecules are bound at a particular single hydration site, and, third, "symmetrically" implies that the two equivalent sites are occupied bilaterally, so hydrated dimers maintain the 2-fold rotational symmetry.

With given mono- or dihydrated neutral $\xi\xi'$ dimer structures, we checked out the possibilities of hydrogen transfer of H_3 or H_3' in the region of the double hydrogen bond between the two adenine monomers, but only to confirm that such hydrogen-transferred structures are considerably less stable in neutral states.

B. Ionization Energies. Next, we consider the ionization energies of hydrated dimers $A_2(H_2O)_n$ ($n = 0-2$) that lead to hydrated adenine dimer ions $A_2^+(H_2O)_n$. Vertical ionization energies (IEs) are calculated as energy differences between the neutral and ionic states of the hydrated adenine dimer structures optimized at the neutral states, as listed in Table 1. Vertical IEs of hydrated dimers are less than 8.0 eV in most cases, as experimentally observed by Kim et al.[41] The bare dimer $\xi\xi'$ has the vertical IE = 7.76 eV, which is considerably smaller than 8.25 eV of a single adenine molecule we obtained at the same level of theory.[42] Vertical IEs of mono- and dihydrated adenine dimers appear to fluctuate near the vertical IE value of the bare dimer, reflecting small differences in hydration effects between the ionic and neutral states at the Franck−Condon regions.

We also calculated the adiabatic IEs as we optimized the structures of hydrated adenine dimer ions, listed in the third and fourth columns of Table 1. (See Figures 2−6 for the optimized structures of hydrated adenine dimer ions.) In general, the adiabatic IEs for un-, mono-, and dihydrated adenine dimers are smaller than their vertical counterparts by at least 0.1 eV. In photoexcitation experiments, the differences in the vertical and adiabatic IEs may be converted to internal energies via structural changes from the Franck−Condon regions to the energy minima of hydrated dimer ions. Larger differences observed in μ-$\xi\xi'$, $\mu\nu$-$\xi\xi'$, $\nu\mu'$-$\xi\xi'$, and $\mu\mu'$-$\xi\xi'$ arise from the fact that a single water molecule bound at the μ or μ' site experiences significant reorientation to reach the energy minima. Note that having two such water molecules leads to the largest difference between the vertical and adiabatic IEs of $\mu\mu'$-$\xi\xi'$. It should be noted, however, that ν is still a more effective hydration site in stabilizing the dimer ion in the potential minimum regime, as the optimized dimer ions, ν-$\xi\xi'^+$, $\nu\nu$-$\xi\xi'^+$, and $\nu\nu'$-$\xi\xi'^+$, are lower in energy than the dimer ions μ-$\xi\xi'^+$, $\mu\mu$-$\xi\xi'^+$, and $\mu\mu'$-$\xi\xi'^+$. Note that we added the superscript + to represent ion species explicitly. However, we will drop it for shorter notations as we discuss the ionic species only hereafter.

C. Intradimer Proton Transfer. Though optimized, the structures of adenine dimer ions, with each adenine monomer structurally intact, are expected to be metastable, because the electron density is depleted mostly from the two remote azine nitrogen atoms (N_9 and N_9') upon ionization, so the single positive charge is near equally divided between the two chemically distinct species, i.e., two adenine monomers each of which is half-charged. It is well-studied by Zhanpeisov and Leszczynski that, in one-electron-oxidized dimer complexes, the interaction between a cation and a radical is energetically more favorable than that between the symmetrical fragments both positively and equally charged.[43]

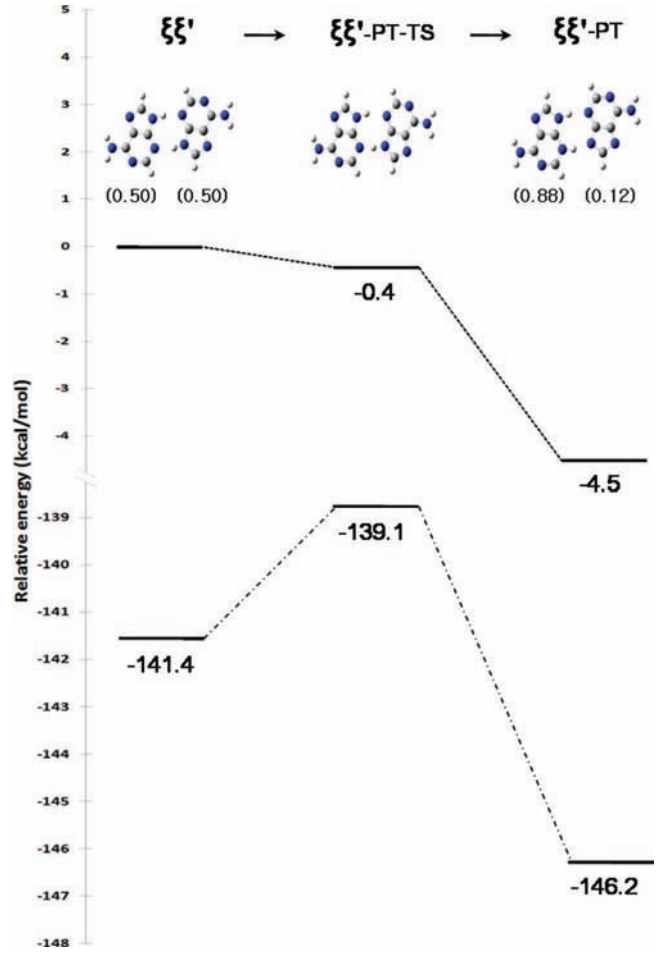

Figure 2. Relative energy diagrams (in kcal/mol) along the H_3 proton transfer reaction coordinate of adenine dimer ion, $\xi\xi'$. The top diagram represents energy profiles with zero-point vibration energies included, while the bottom one shows the electronic energies only. NBO charges of distinct adenine moieties are shown before and after proton transfer. The origin of the vertical energy scale refers to the energy of optimized dimer ion listed in the last column of Table 1.

Figure 2 shows the unhydrated dimer ion $\xi\xi'$ undergoing H_3 proton transfer. In the bottom of Figure 2, the relative energy diagram compares only the electronic energies of the initial adenine dimer ion $\xi\xi'$, the proton-transferred dimer ion ($\xi\xi'$-PT), and the transition state ($\xi\xi'$-PT-TS), of which the relationship was confirmed with IRC calculation. (The suffix PT stands for proton transferred and the other suffix TS is added to represent the transition state leading to the corresponding product. This convention will be used throughout this work.) The diagram appears to be a typical unimolecular reaction over a barrier toward the product, but the barrier nearly disappears as we make corrections for electronic energies with zero-point harmonic vibrations. With zero-point vibrational energies included, the energy of reactant $\xi\xi'$ becomes higher than that of the electronic transition state $\xi\xi'$-PT-TS, which is still kept higher than that of the product $\xi\xi'$-PT. It implies that the proton-transferred structure $\xi\xi'$-PT can be easily reached, helped by some minimal vibrational motions. IRC calculation verifies that the barrier at 0 K is less than 0.5 kcal/mol (Figure S3, Supporting Information). Note that the internal energy increase after the proton transfer will be 4.5 kcal/mol, on the same order of magnitude as the energy to be obtained via geometry relaxations from the neutral to the ionic dimer structures, 2.0 kcal/mol, after

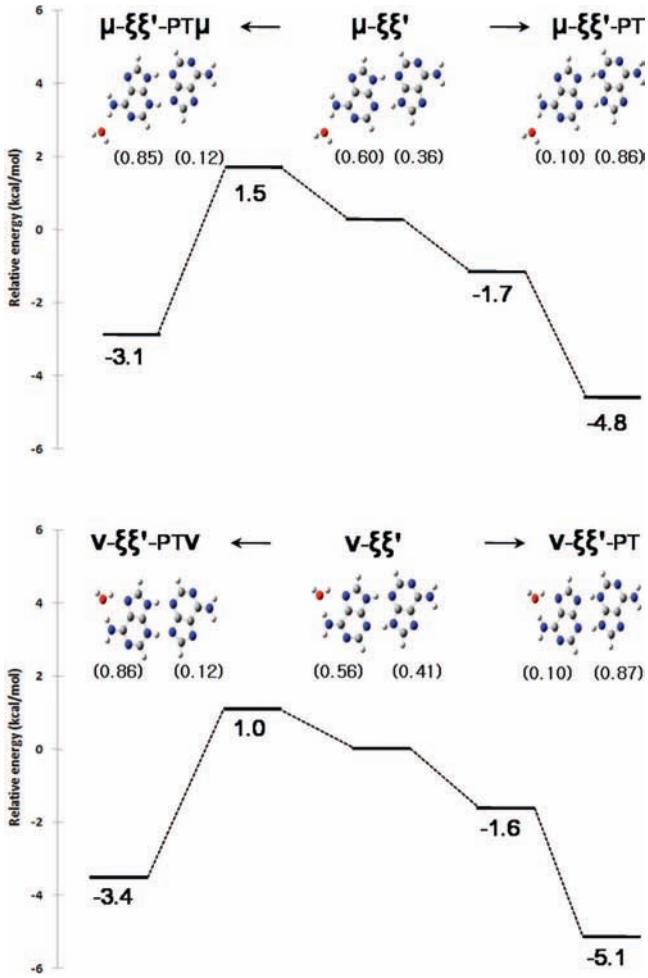

Figure 3. Relative energy diagram (in kcal/mol) along the H_3 proton transfer reaction coordinate of adenine dimer ion, when the dimer ion is monohydrated at μ and ν sites, respectively. The two dimer ions are called μ-$\xi\xi'$ and ν-$\xi\xi'$, and relative energies shown are corrected with zero-point vibrations. NBO charges of distinct adenine moieties are shown before and after proton transfer. The origin of the vertical energy scale refers to the energy of optimized dimer ion listed in the last column of Table 1.

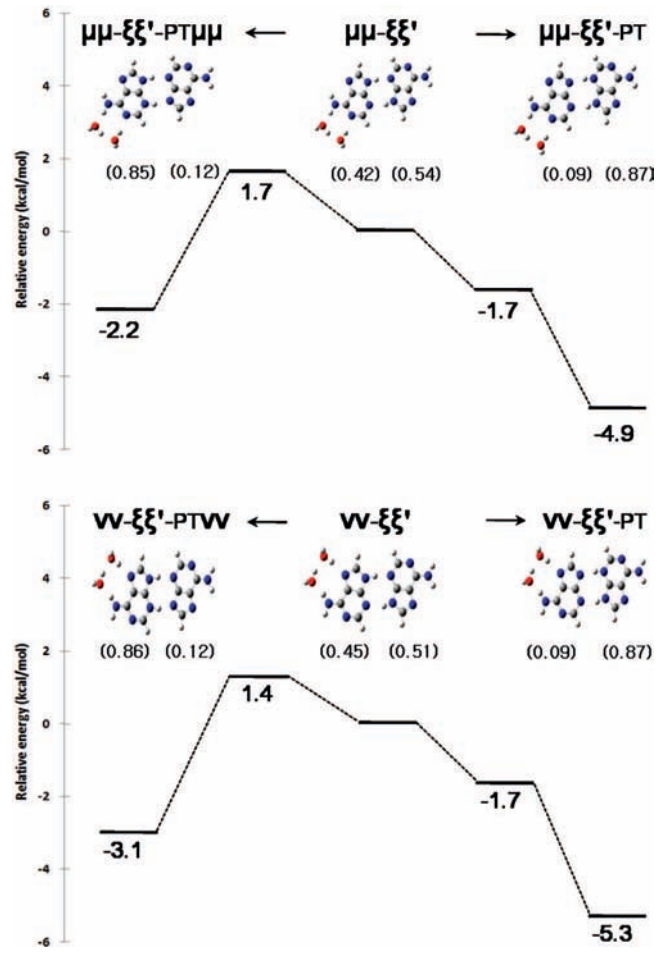

Figure 4. Relative energy diagram (in kcal/mol) along the H_3 proton transfer reaction coordinate of adenine dimer ion, when the dimer ion is unilaterally and doubly dihydrated at μ and ν sites, respectively. The two dimer ions are called $\mu\mu$-$\xi\xi'$ and $\nu\nu$-$\xi\xi'$, and relative energies shown are corrected with zero-point vibrations. NBO charges of distinct adenine moieties are shown before and after proton transfer. The origin of the vertical energy scale refers to the energy of optimized dimer ion listed in the last column of Table 1.

the vertical ionization. The observation that there is virtually no barrier at 0 K and that the thermodynamically stable structures are the proton-transferred ones will be repeatedly found as we move along to hydration cases as well. As ionization occurs vertically in experiments, hydrated dimer ions will have practically enough internal energy to trigger the proton transfer.

Natural population analysis was performed to assign the NBO charge to each atom in the dimer ions. In Figure 2, the NBO atomic charges are summed over each distinct species in the hydrogen-bonded dimer ions. The initial dimer structure has 50:50 charge separation between the two adenine moieties, but the proton-transferred product has a considerable charge disproportion, 88:12, toward the one with hydrogen atom added, suggesting that the reaction is characterized, indeed, as proton transfer, not hydrogen-transfer.

To move on to monohydrated dimer ion cases, Figure 3 (top) shows the zero-point vibration corrected relative energies of the proton-transferred products and the transition-state molecular configurations associated with them, when the μ site is occupied with a water molecule. Monohydration breaks the 2-fold rotational symmetry of the dimer ion structure, so there are two reaction pathways available for proton transfer. One way is for a proton to transfer to unhydrated adenine moiety, of which the relative potential energy profile looks very similar to the bare dimer ion case. The other is for another proton to proceed to the hydrated moiety, in which the proton must surmount the transition-state barrier of 1.5 kcal/mol to the product. Note that this energy barrier is small enough that the internal energy gain from geometry relaxations after the vertical ionization may help push the reaction in this direction. The ν-site monohydration exhibits very similar reaction schemes, but the stabilization energies due to proton transfer are about 0.3 kcal/mol larger than the μ-site monohydration. The transition-state barrier toward hydrated adenine moiety is ~0.5 kcal/mol lower in ν-site monohydration. As in the bare dimer ion, the NBO charge analysis illustrates that the single positive charge, near evenly divided between the adenine molecules before proton transfer, becomes shifted to protonated adenine ions in the proton-transferred adenine dimer ions. The charges of water molecules are a few hundredths of an atomic unit and are omitted in Figure 3 for simplicity.

When we have two water molecules in μ or ν site in doubly dihydration cases (Figure 4), the directional preference in proton transfer appears the same way as in monohydration cases. However, the tendency of proton transferring to unhydrated adenine moiety becomes stronger in both kinetic and thermo-

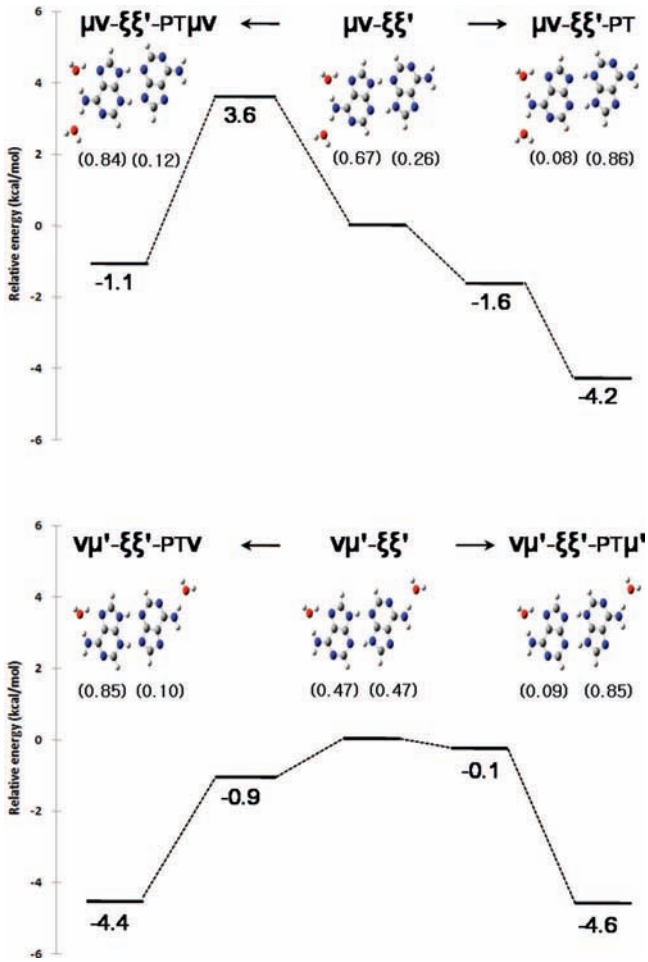

Figure 5. Relative energy diagram (in kcal/mol) along the H_3 proton transfer reaction coordinate of adenine dimer ion, when the dimer ion is unilaterally and bilaterally dihydrated at μ and ν sites, respectively. The dimer ions are called $\mu\nu$-$\xi\xi'$ and $\nu\mu'$-$\xi\xi'$, and relative energies shown are corrected with zero-point vibrations. NBO charges of distinct adenine moieties are shown before and after proton transfer. The origin of the vertical energy scale refers to the energy of optimized dimer ion listed in the last column of Table 1.

dynamic perspectives. Comparing $\nu\nu$-$\xi\xi'$ with $\mu\mu$-$\xi\xi'$, we see that the ν site is more effective in terms of stabilizing the proton-transferred products and reducing the transition-state barrier of proton transferring to hydrated adenine moiety. Again, the NBO charges are summed over each distinct molecular species in the hydrogen-bonded dimer ions in Figure 4, showing that the reactions are characterized as proton transfer.

In Figure 5, the dimer ions are unilaterally (top) and bilaterally (bottom) dihydrated at the two unequivalent sites, respectively. When the two sites, μ and ν, of one adenine moiety are occupied with water molecules, proton transfer looks significantly biased to the unhydrated adenine moiety. The proton transfer to the dihydrated adenine moiety is unfavorable, because the transition state, $\mu\nu$-$\xi\xi'$-PT$\mu\nu$-TS, is raised to 3.6 kcal/mol, and also the product, $\mu\nu$-$\xi\xi'$-PT$\mu\nu$, is only 1 kcal/mol more stable than the reactant. Apparently, having two water molecules bound at the two different sites μ and ν of one adenine moiety results in larger proton transfer preference than the previous hydrations. When the two unequivalent sites, ν and μ', belonging to the different adenine moieties, are occupied, the directional preference in proton transfer almost disappears as shown in the bottom of Figure 5. Earlier in Figure 3, we found a tendency for monohydration to prefer proton transfer to unhydrated adenine moiety, i.e., monohydrated moiety giving away a proton to the unhydrated other. The $\nu\mu'$-$\xi\xi'$ case is a direct comparison of the tendencies of two different monohydrations, although only a very small difference is exhibited.

Figure 6 illustrates the proton transfer when two water molecules are initially bound symmetrically at the equivalent positions of the adenine dimer ion, $\mu\mu'$-$\xi\xi'$ and $\nu\nu'$-$\xi\xi'$. The symmetry lets us consider one-way proton transfer only, as in the bare dimer ion case, $\xi\xi'$. We find that the proton-transferred product ν'-$\xi\xi'$-PTν is more stable than $\mu\mu'$-$\xi\xi'$-PTμ, confirming again that ν is the more effective hydration site.

In all proton-transferred products above, it should be noted that AH^+ is not a uniformly charged ion but a 16-atom species of which most charge is concentrated in the double hydrogen-bond region. Therefore, typical ion−dipole interactions that would make the dimer products of type $(A-H)-(AH^+)\cdot(H_2O)_n$ more stable than the other $(H_2O)_n\cdot(A-H)-(AH^+)$ are not necessarily a dominant factor in determining the energetics. Also, the energy profiles in Figures 3-6 provide only the local picture of potential energy surfaces near the intradimer proton transfer regime. Here we did not search for the global minima of the final product structures that may involve rearrangements of water molecules in complexes, since the main goal in this work is to estimate the hydration effects on the proton transfer that occurs immediately after ionization.

One may think that more realistic hydrations with three or more water molecules involve, in general, both adenine molecules of the dimer, because water molecules being crowded at a single adenine moiety will be rather rare events even in gas-phase environments. In any such rare asymmetric cases, however, the directional preference in proton transfer should arise from hydration-induced asymmetry in the already metastable electron density of the dimer ion. Effects of generally asymmetric (or unilateral at the extreme) hydrations serve to push a proton from hydrated to less hydrated (or unhydrated at the extreme) adenine.

To investigate asymmetric hydration effects further, we compared the NBO charges of six atoms participating in double hydrogen bonds between the two adenine moieties, before proton transfer takes place. (top of Figure 7) First, it is found that the charges on the proton-donor groups (N_9-H_3 or $N_9'-H_3'$) are kept nearly unchanged. The hydrogen and nitrogen charges are not much affected by hydrations, maintained at around 0.47 and −0.58, respectively. However, the charges of proton-acceptor atoms, N_3 and N_3', become differentiated as hydration concentrates on one adenine molecule. As only one adenine (unprimed) moiety in the dimer ions is hydrated, the N_3 charge of that adenine moiety becomes significantly less negative, i.e., −0.524 (μ-$\xi\xi'$), −0.527 (ν-$\xi\xi'$), −0.528 ($\mu\mu$-$\xi\xi'$), −0.521 ($\nu\nu$-$\xi\xi'$), and −0.502 ($\mu\nu$-$\xi\xi'$), implying that water molecules withdraw the electron density near the N_3 atom and lessen its basicity. On the other hand, the N_3' charge of the other adenine moiety becomes more negative to the same extent as the N_3 charge is less negative, so its basicity is enhanced. The bottom of Figure 7 illustrates how the charges of the two proton acceptors, N_3 and N_3', are related to the transition-state energies. For *asymmetric* hydration cases, the transition-state energy differences between the two kinds of proton transfer are plotted against the proton-acceptor charge differences. Note that the six data points are quite close to the linear regression line. It tells us that the more asymmetric proton transfer will be kinetically induced, as hydrations become more asymmetric and this make the charges of proton-acceptors more differentiated. Interestingly, μ-site hydration cases, μ-$\xi\xi'$ and $\mu\mu$-$\xi\xi'$, lead to a little bit larger transition-state energy differences than ν-site coun-

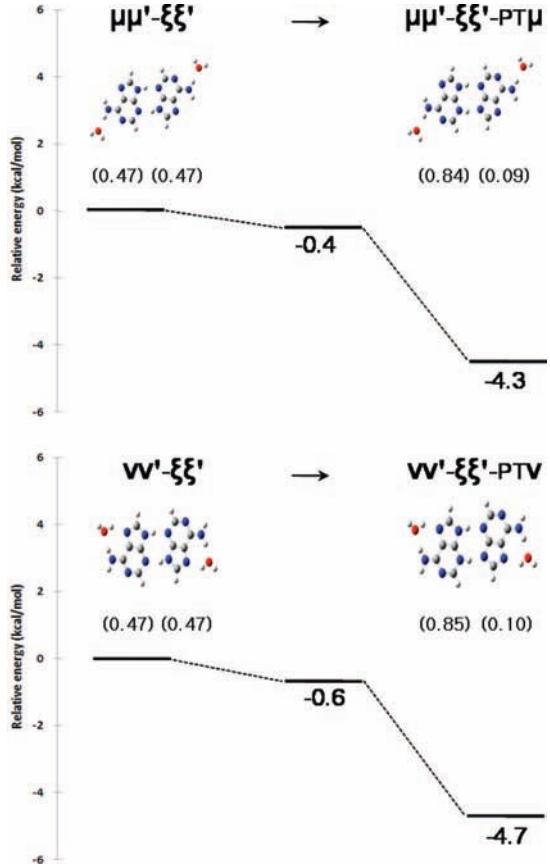

Figure 6. Relative energy diagram (in kcal/mol) along the H_3 proton transfer reaction coordinate of adenine dimer ion, when the dimer ion is bilaterally symmetrically dihydrated at μ or ν sites, respectively. The two dimer ions are called $\mu\mu'$-$\xi\xi'$ and $\nu\nu'$-$\xi\xi'$, and relative energies shown are corrected with zero-point vibrations. NBO charges of distinct adenine moieties are shown before and after proton transfer. The origin of the vertical energy scale refers to the energy of optimized dimer ion listed in the last column of Table 1.

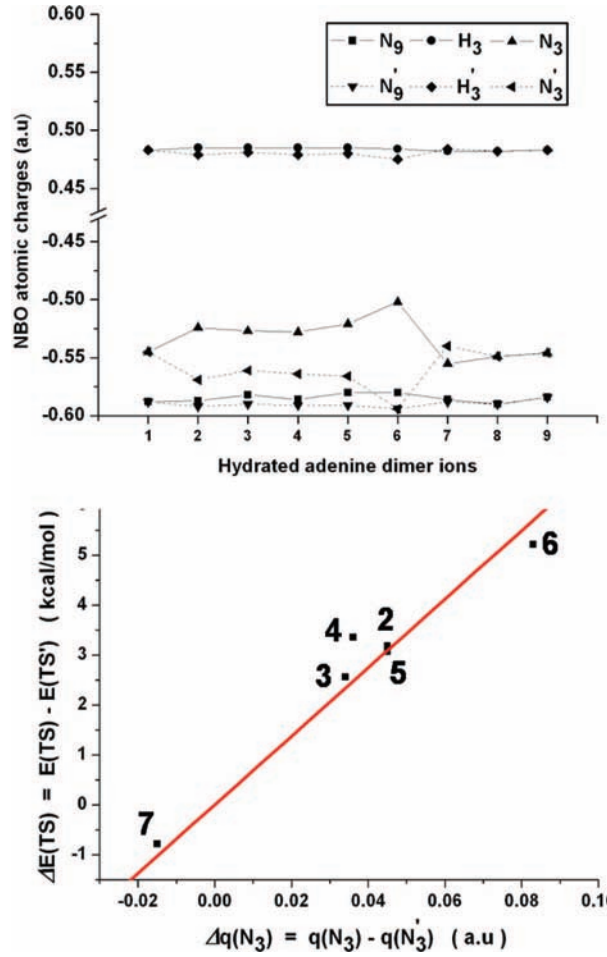

Figure 7. (Top) The NBO charges (in au) of six atoms at the region of the double hydrogen bond are shown for nine different un-, mono-, and dihydrated dimer ions, which are numbered as (1) $\xi\xi'$, (2) μ-$\xi\xi'$, (3) ν-$\xi\xi'$, (4) $\mu\mu$-$\xi\xi'$, (5) $\nu\nu$-$\xi\xi'$, (6) $\mu\nu$-$\xi\xi'$ (7), $\nu\mu'$-$\xi\xi'$, (8) $\mu\mu'$-$\xi\xi'$, and (9) $\nu\nu'$-$\xi\xi'$. (Bottom) The transition-state energy differences between the two unequivalent proton transfers for six asymmetrically hydrated adenine dimer ions, (2) μ-$\xi\xi$, (3) ν-$\xi\xi'$, (4) $\mu\mu$-$\xi\xi'$, (5) $\nu\nu$-$\xi\xi'$, (6) $\mu\nu$-$\xi\xi'$, and (7) $\nu\mu'$-$\xi\xi'$, are plotted against the NBO charge differences between N_3 and N_3'.

terparts, ν-$\xi\xi'$, and $\nu\nu$-$\xi\xi'$, implying that μ-site hydration is kinetically a little more effective in differentiating proton-acceptors and biasing proton transfer. In the $\nu\mu'$-$\xi\xi'$ case, proton transfer occurs near barrierless in either direction, but the downhill slope to the ν-site monohydrated adenine moiety appears a little bit steeper than the slope to the μ-site monohydrated adenine moiety. It is noticeable that, in the $\mu\nu$-$\xi\xi'$ case, the asymmetry in proton transfer is maximized due to cooperative hydration effects at both μ and ν sites on proton-acceptor charge differentiation.

Our finding that the charge of the proton-accepting N_3 varies upon hydration is something that is not observed in hydrated single adenine molecules or their ions. Separate calculations of hydration effects on a single adenine molecule and its ion confirm that N_3 charge variations due to hydration at μ or ν are minimal (Figures S4 and S5, Supporting Information). Therefore, it can be characterized as a unique property from the dimer ion formation. Also, similar properties are anticipated from other double-hydrogen-bonded dimer ions of types like $\xi\mu'$, $\xi\nu'$, $\mu\mu'$, $\nu\mu'$, and $\nu\nu'$, which are not discussed in this work.

D. Dimer Cleavage vs Evaporation of Water Molecules. According to our calculations, hydrated adenine dimer ions undergo very easy proton transfer after ionization. Then, the proton-transferred hydrated dimer ions may be tested for their stability using photoexcitations or induced collisions.

Detailed dynamics leading to photofragmentation products depends on which molecular species serves as a chromophore at a particular wavelength, and a fair understanding requires a sufficient knowledge of many difficult topics such as excited-state energies, intramolecular relaxations, internal conversion, and intersystem crossing. To have a clue on how photofragmentations are started, though, we can briefly consider dissociative processes after the system returns to the ground-state potential energy surface, assuming that the role of photoexcitation is limited to providing extra internal energy.

In fact, the major fragment of photodissociation experiments turned out to be the protonated adenine ion AH^+,[12] suggesting that both solvent evaporation and dimer cleavage occurred. One may wonder, therefore, how much energy should be present in hydrated dimer ions, in order for AH^+ to break away from two kinds of molecular species, A−H radical, and water molecules.

In Table 2, we list the energies required for breaking the double hydrogen bonds, i.e., dimer interaction energies, comparing the energies between the proton-transferred hydrated dimer ions and the combined energies of the two separately optimized fragments, $AH^+(H_2O)_m$ and $(A-H)H_2O_{(n-m)}$, $(m \leq n)$. The dimer interaction energy for the bare proton-transferred dimer ion is 30.0 kcal/mol. For hydrated dimer ions, the interaction energies are 1−2 kcal/mol larger than the bare dimer case, because solvation effects on the dimer ion are larger than on resulting

TABLE 2: Dimer Interaction Energies and Threshold Energies for AH^+ Production of Hydrated Proton-Transferred Adenine Dimer Ions[a]

	dimer interaction energy, kcal/mol	threshold energy for AH^+, kcal/mol
$\xi\xi'$-PT	30.0	30.0
μ-$\xi\xi'$-PTμ	29.4	37.3
μ-$\xi\xi'$-PT	32.2	32.2
ν-$\xi\xi'$-PTν	30.8	38.6
ν-$\xi\xi'$-PT	31.0	31.0
$\mu\mu$-$\xi\xi'$-PT$\mu\mu$	30.9	43.2
$\mu\mu$-$\xi\xi'$-PT	30.9	30.9
ν-ν'-PT$\nu\nu$	31.0	44.7
$\nu\nu$-$\xi\xi'$-PT	31.0	31.0
$\mu\nu$-$\xi\xi$-PT$\mu\nu$	29.2	45.1
$\mu\nu$-$\xi\xi'$-PT	32.5	32.5
$\nu\mu'$-$\xi\xi'$-PTν	32.9	40.7
$\nu\mu'$-$\xi\xi'$-PTμ'	30.2	38.1
$\mu\mu'$-$\xi\xi'$-PTμ	31.4	39.3
$\nu\nu'$-$\xi\xi'$-PTν	31.8	39.6

[a] For a proton-transferred hydrated dimer ion, the dimer interaction energy is the energy required only for breaking the double hydrogen bond between the two adenine moieties, and the threshold energy is the minimum energy for taking AH^+ out of the ion. Dimer interaction and threshold energies are calculated with counterpoise corrections.

fragments. Differences in dimer interaction energies of the two kinds of proton-transferred products for a particular hydrated dimer ion arise from the fact that charge-dispersing solvent effects on AH^+ ion are more effective than on the neutral A.

Note that, when the proton transfer takes place to unhydrated moieties, breaking only the double hydrogen bond creates AH^+. For the other cases, it is necessary to break hydrogen bonds between water molecules and the protonated adenine, besides the double hydrogen bonds. We found that about 8 kcal/mol is required additionally for such processes, as summarized in the third column of Table 2.

The thresholds for AH^+ production may be referenced for experimentally removing (A−H) radical and water molecules, but one important question still remains from the viewpoint of dynamics: exactly what do the hydrated adenine dimer ions go through to yield the protonated adenine ion, AH^+? One would expect that the removal of water molecules, i.e., evaporation, does not occur simultaneously with the double hydrogen bond breaking, unless given internal energies are large enough. In fact, with a limited amount of internal energy, evaporation processes are just another reaction competing with the adenine dimer ion cleavage, and there are questions of dynamics, such as which process comes first and how fast either of the two processes can occur.

To compare evaporation with dimer cleavage from energetics perspective, we calculated the hydration energies as water molecules are removed one after another from hydrated adenine dimer ions, by taking differences in the energies of optimized hydrated adenine dimer ions shown in Figures 2−6 (Figures S6 and S7, Supporting Information) Interestingly, hydration energies do not depend much on whether the proton transfer has occurred or not, and single-molecule evaporation processes cost nearly constant (8 ± 1 kcal/mol) energies, although it is confirmed that ν is a stronger hydrogen-bonding site and the last water molecule is harder to remove than the previous ones. As in our previous photodissociation experiments,[12] use of different excitation wavelengths could control the degree of evaporation and dimer cleavage. For instance, upon photoexcitation at a long wavelength of 532 nm, only small hydrated clusters, $[(AH^+)-(A-H)](H_2O)_n$ ($n < 3$), are expected to dissociate into AH^+ and other fragments. However, in order to investigate more detailed dynamics of both evaporation and dimer cleavage in particular experimental conditions, it would be necessary to do a separate theoretical study such as the RRKM calculation or MD simulation at the ground-state potential energy surface.

VI. Concluding Remarks

We found the mono- and dihydration patterns for adenine dimer molecules and their ions and confirmed that the ν-site hydration is effective for stabilizing them. The ionization energies of hydrated adenine dimers were calculated around 7.8 eV.

According to our calculations, upon ionization, intradimer proton transfers readily occur with negligible barriers in normal hydration conditions. However, when hydration patterns are unilateral or asymmetric, proton transfers to the hydrated adenine moiety are kinetically hindered due to the transition-state barrier elevated as high as 1−2 kcal/mol. There, μ-site hydration introduces more of such kinetic hindrance than ν-site. A very strong directional preference in proton transfer was observed in the case of $\mu\nu$-site unilateral dihydration, because of the very high transition-state energy, 3.6 kcal/mol. It turns out that the directional preference in proton transfer arises from the charge differentiation of proton-accepting nitrogen atoms of dimer ions due to asymmetric hydration, which may be characterized as a unique dimer ion property.

The cleavage of dimer structure in hydrated dimer ions needs about 30 kcal/mol, whereas the evaporation of each water molecule requires just 8 kcal/mol or so. It suggests that, with a limited amount of internal energy available, evaporation processes may precede dimer cleavages.

The detailed dynamics study of photofragmentation processes should rely upon ab initio molecular dynamics simulations. Currently, we are investigating which molecular species of dimer ions serve as a chromophore in various photoexcitation conditions.

Acknowledgment. This work was supported by the Korea Research Foundation Grant funded by the Korean Government (MOEHRD, Basic Research Promotion Fund, KRF-2006-311-C00078) S.M.P. and S.R. are very grateful to Hye Yeon Kim for helpful discussions.

Supporting Information Available: Optimized geometries at the B3LYP/6-31+G(d,p) level of six adenine dimer structures, adenine molecule, and its hydrated ions are included. IRC calculation result for unhydrated adenine dimer ion and hydration energies at hydrated adenine dimer ions are showed. Also, Cartesian coordinates of optimized structures of hydrated dimer ions in Figures 2−6 are listed. This material is available free of charge via the Internet at http://pubs.acs.org.

References and Notes

(1) Callis, P. R. *Annu. Rev. Phys. Chem.* **1983**, *34*, 329.

(2) Shukla, M. K.; Leszczynski, J. In *Computational Chemistry: Reviews of Current Trends*; Leszczynski, J. Ed.; World Scientific: River Edge, NJ, 2003; Vol. 8, pp 249−343.

(3) Crespo-Hernández, C. E.; Cohen, B.; Hare, P. M.; Kohler, B. *Chem. Rev.* **2004**, *104*, 1977.

(4) Pecourt, J.-M. L.; Peon, J.; Kohler, B. *J. Am. Chem. Soc.* **2000**, *122*, 9348.

(5) Pecourt, J.-M. L.; Peon, J.; Kohler, B. *J. Am. Chem. Soc.* **2001**, *123*, 10370.

(6) Peon, J.; Zewail, A. H. *Chem. Phys. Lett.* **2001**, *348*, 255.
(7) Kang, H.; Lee, K. T.; Jung, B.; Ko, Y. J.; Kim, S. K. *J. Am. Chem. Soc.* **2002**, *124*, 12958.
(8) Plützer, C.; Hünig, I.; Kleinermanns, K. *Phys. Chem. Chem. Phys.* **2003**, *5*, 1158.
(9) Kelly, R. E. A.; Lee, Y. J.; Kantorovich, L. N. *J. Phys. Chem. B* **2005**, *109*, 11933.
(10) Amo-Ochoa, P.; Alexandre, S. S.; Pastor, C.; Zamora, F. *J. Inorg. Biochem.* **2005**, *99*, 2226.
(11) Ritze, H.-H.; Lippert, H.; Samoylova, E.; Smith, V. R.; Hertel, I. V.; Radloff, W.; Schultz, T. *J. Chem. Phys.* **2005**, *122*, 224320.
(12) Nam, S. H.; Park, H. S.; Ryu, S.; Song, J. K.; Park, S. M. *Chem. Phys. Lett.* **2008**, *450*, 236.
(13) Perun, S.; Sobolewski, A. L.; Domcke, W. *J. Am. Chem. Soc.* **2005**, *127*, 6257.
(14) Marian, C. M. *J. Chem. Phys.* **2005**, *122*, 104314.
(15) Blancafort, L. *J. Am. Chem. Soc.* **2006**, *128*, 210.
(16) Serrano-Andrés, L.; Merchán, M.; Borin, A. C. *Proc. Natl. Acad. Sci.U.S.A.* **2006**, *103*, 8691.
(17) Cohen, B.; Hare, P. M.; Kohler, B. *J. Am. Chem. Soc.* **2003**, *125*, 13594.
(18) Ullrich, S.; Schultz, T.; Zgierski, M. Z.; Stolow, A. *J. Am. Chem. Soc.* **2004**, *126*, 2262.
(19) Samoylova, E.; Lippert, H.; Ullrich, S.; Hertel, I. V.; Radloff, W.; Schultz, T. *J. Am. Chem. Soc.* **2005**, *127*, 1782.
(20) Satzger, H.; Townsend, D.; Zgierski, M. Z.; Patchkovskii, S.; Ullrich, S.; Stolow, A. *Proc. Nat. Acad. Sci.U.S.A.* **2006**, *103*, 10196.
(21) Löwdin, P. D. *Adv. Quantum Chem.* **1965**, *2*, 213.
(22) Nelson, C. C.; McCloskey, J. A. *J. Am. Chem. Soc.* **1992**, *114*, 3661.
(23) Marian, C.; Nolting, D.; Weinkauf, R. *Phys. Chem. Chem. Phys.* **2005**, *7*, 3306.
(24) Tureèek, F.; Chen, X. *J. Am. Soc. Mass. Spectrom* **2005**, *16*, 1713.
(25) Hünig, I.; Plützer, C.; Seefeld, K. A.; Löwenichv, D.; Nispel, M.; Kleinermanns, K. *Chem. Phys. Chem.* **2004**, *5*, 1427.
(26) Schinke, R. *Photodissociation Dynamics, Cambridge Monographs on Atomic, Molecular, and Chemical Physics*; Cambridge University Press; London, 1995.
(27) Marx, D.; Hutter, J. *Ab Initio Molecular Dynamics; Theory and Implementation, in Modern Methods and Algorithms of Quantum Chemistry; Preceedings*, 2nd ed.; NIC Series 3; John von Newmann Institute for Computing: Julich, Switzerland, 2000; pp 301−449.
(28) Langer, H.; Doltsinis, N. L. *Phys. Chem. Chem. Phys.* **2003**, *5*, 4516.
(29) Nam, S. H.; Park, H. S.; Song, J. K.; Park, S. M. *J. Phys. Chem. A* **2007**, *111*, 3480.
(30) Nam, S. H.; Park, H. S.; Ryu, S.; Song, J. K.; Park, S. M. In preparation.
(31) Frisch, M. J.; Trucks, G. W.; Schlegel, H. B.; Scuseria, G. E.; Robb,M. A.; Cheeseman, J. R.; Montgomery, J. A.; Vreven, T.; Kudin, K. N.; Burant, J. C.; Millam, J. M.; Iyengar, S.; Tomasi, J.; Barone, V.; Mennucci, B.; Cossi, M.; Scalmani, G.; Rega, N.; Petersson, G. A.; Nakatsuji, H. ;Hada, M.; Ehara, M.; Toyota, K.; Fukuda, R.; Hasegawa, J.; Ishida, M. ; Nakajima, T.; Honda, Y.; Kitao, O.; Nakai, H.; Klene, M.; Li, X.; Knox, J. E.; Hratchian, H. P.; Cross, J. B.; Adamo, C.; Jaramillo, J.; Gomperts, R. ;Stratmann, R. E.; Yazyev, O.; Austin, A. J.; Cammi, R.; Pomelli, C.; Ochterski, J.; Ayala, P. Y.; Morokuma, K.; Voth, G. A.; Salvador, P.; Dannenberg, J. J.; Zakrzewski, V. G.; Dapprich, S.; Daniels, A. D.; Strain,M. C.; Farkas, O.; Malick, D. K.; Rabuck, A. D.; Raghavachari, K.; Foresman, J. B.; Ortiz, J. V.; Cui, Q.; Baboul, A. G.; Clifford, S.; Cioslowski, J.; Stefanov, B. B.; Liu, G.; Liashenko, A.; Piskorz, P.; Komaromi, I.; Martin, R. L.; Fox, D. J.; Keith, T.; Al-Laham, M. A.; Peng, C. Y.; Nanayakkara, A.; Challacombe, M.; Gill, P. M. W.; Johnson, B.; Chen,W.; Wong, M. W.; Andres, J. L.; Gonzalez, C.; Replogle, E. S.; Pople, J. A. *Gaussian 03, rev. C.02*; Gaussian, Inc.: Pittsburgh, PA, 2003.
(32) Glendening, E. D.; Reed, A. E.; Carpenter, J. E.; Weinhold, F. *NBO version 3.1*.
(33) Boys, S. F.; Bernardi, F. *Mol. Phys.* **1970**, *19*, 553.
(34) Carles, S.; Lecomte, C. F.; Schermann, J. P.; Desfrançois, C. *J. Phys. Chem. A* **2000**, *104*, 10662.
(35) Sukhanov, O. S.; Shishkin, O. V.; Gorb, L.; Podolyan, Y.; Leszczynski, J. *J. Phys. Chem. B* **2003**, *107*, 2846.
(36) Chandra, A. K.; Nguyen, M. T.; Uchimaru, T.; Zeegers-Huyskens, T. *J. Phys. Chem. A* **1999**, *103*, 8853.
(37) Kim, H.-T. *J. Mol. Struct. (THEOCHEM)* **2004**, *673*, 121.
(38) Jalbout, A. F.; Adamowicz, L. *J. Phys. Chem. A* **2001**, *105*, 1033.
(39) Hanus, M.; Kabeláč, M.; Rejnek, J.; Ryjáček, F.; Hobza, P. *J. Phys. Chem. B* **2004**, *108*, 2087.
(40) McConnell, T. L.; Wheaton, C. A.; Hunter, K. C.; Wetmore, S. D. *J. Phys. Chem. A* **2005**, *109*, 6351.
(41) Kim, S. K.; Lee, W.; Herschbach, D. R. *J. Phys. Chem.* **1996**, *100*, 7933.
(42) The vertical experimental ionization energy was reported as 8.44 eV (Lin, J.; Yu, C.; Peng, S.; Akiyama, I.; Li, K.; Lee, L. K.; Lebreton, P. R. *J. Am. Chem. Soc.* **1980**, *102*, 4627) , while the previous B3LYP calculation with 6-31++G(d,p) (Close, D. M. *J. Phys. Chem.* **2004**, *108*, 10376) results in 8.26 eV, which is similar to 8.25 eV of the current work.
(43) Zhanpeisov, N. U.; Leszczynski, J. *J. Phys. Chem. A* **1999**, *103*, 8317.

JP801238B